

Upper bounds of spin-density wave energies in the homogeneous electron gas

F. Delyon,^{1,2} B. Bernu,² L. Baguet,² and M. Holzmann^{2,3}

¹CPHT, UMR 7644 of CNRS, École Polytechnique, F-91128 Palaiseau Cedex, France

²LPTMC, UMR 7600 of CNRS, UPMC, Paris-Sorbonne, F-75252 Paris Cedex 05, France

³LPMMC, UMR 5493 of CNRS, Université J. Fourier, BP 166, F-38042 Grenoble Cedex, France

Studying the jellium model in the Hartree-Fock approximation, Overhauser has shown that spin density waves (SDW) can lower the energy of the Fermi gas, but it is still unknown if these SDW are actually relevant for the phase diagram. In this paper, we give a more complete description of SDW states. We show that a modification of the Overhauser ansatz explains the behavior of the jellium at high density compatible with previous Hartree-Fock simulations.

PACS numbers: 71.10.-w, 71.10.Ca, 71.10.Hf, 71.30.+h, 03.67.Ac

The simplest model of electronic structure is jellium – electrons embedded in a homogeneous background of opposite charge such that the system is neutral. This model is a good starting point to describe properties of simple metals such as sodium[1]. At zero temperature, the only parameter of this model is the density n , or the dimensionless parameter $r_s = 3/(4\pi n a_B^3)^{1/3}$, where $a_B = \hbar^2/(me^2)$ is the Bohr radius. Within the Hartree-Fock approximation (HF), Overhauser has shown that the Fermi gas is unstable under a spin density wave (SDW)[2, 3]. Only recently, almost 50 years after Overhauser’s prediction, explicit numerical estimates of the HF ground state have shown SDW evidences of the electron gas in three[4–7] and two dimensions[7, 8]. Still, a quantitative estimate of the variation of the SDW amplitude and energy in the high density region $r_s \lesssim 1$ is missing[9]. In this letter, we generalize Overhauser’s ansatz and provide a quantitative solution of this long-standing problem.

The key point is to search for a solution in a non-perturbative way. Indeed, small domains exist around the Fermi surface where the one-body states differ radically from a single plane wave. These states of wave vector \mathbf{k} are coupled with the wave vector $\mathbf{k} + \mathbf{Q}_\mathbf{k}$ where $\mathbf{Q}_\mathbf{k}$ is constant over each domain. The larger is this domain, the larger will be the energy gain of the SDWs. One way to enlarge this domain is to cut the top of sphere as explained by Overhauser[2]. In the following we show that adding a small cylinder on the top of the truncated sphere as shown in Fig.1 can increase the energy gain of the SDW by orders of magnitude compared to Overhauser’s ansatz. Furthermore, we provide an explicit estimate of the energy gain of the SDW state. As we will see, the optimal size of these domains dramatically shrinks with increasing density, resulting in a extremely rapid decrease of the tiny SDW energy gain and explaining the difficulties of observing SDW in the high density region.

Our semi-analytical results presented here are compared to recent HF results[6] obtained with periodic models. Indeed, the Overhauser’s ansatz is in fact a periodic model (a crystal where the one-body states are limited

to the first mode) as soon as the set vectors $\mathbf{Q}_\mathbf{k}$ belong to a discrete lattice. As the density increases the number of vectors $\mathbf{Q}_\mathbf{k}$ (and of domains around the Fermi sphere) may also increases[2] leading to a quasi-crystal which cannot be describe by a periodic model.

Let us mention that in this paper we focus on the SDW states. These states are easier to compute leading to simpler formulas since the density of charge is constant. Equivalent results may be obtained[2, 3] for the charge density waves (CDW).

In the following, we outline the main steps in the calculation of the SDW energies. First we introduce the deformation of the Fermi surface generalizing Overhauser’s model and describe the SDW ansatz for the single particle states. We then show how the optimal solution can be found by calculating the fixed point solution of a non-linear functional equation. The explicit results are then obtained by restricting to a one dimensional function and compared to the outcome of previous numerical simulations.

Fermi gas energy of the truncated sphere. Let us call E_{FG} the HF-energy of the Fermi gas where only plane wave states of wave vectors \mathbf{k} inside the Fermi sphere of radius k_F are occupied. Following Overhauser, in a first step the Fermi sphere is deformed into a volume \mathcal{F} as shown in Fig.1, and its energy increase is denoted $\Delta E_{\text{FG}}^{\mathcal{F}} = E_{\text{FG}}^{\mathcal{F}} - E_{\text{FG}}$. Here, the subscript FG is used to point out that the many-body state is a Slater determinant of plane wave states inside the corresponding Fermi surface. Using k_F as unit of wave vectors, the sphere in Fig.1 has unit radius, and the deformation is characterised by a small parameter ϵ approaching zero as r_s decreases. In order to keep the electron density constant, the deformed surface in the figure must be scaled by R [11] such that $R^3 \int_{\mathcal{F}_R} d\mathbf{k} = R^3 \int_{\mathcal{F}_1} d\mathbf{k} = 4\pi/3$. The Fermi gas energy per particle in Hartree units ($Ha =$

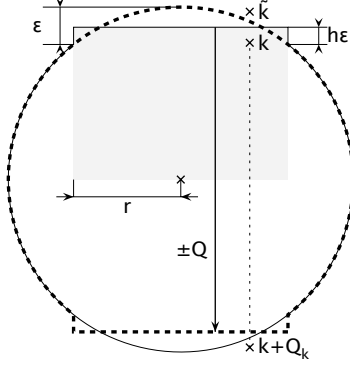


FIG. 1: Shape of occupied zones for spiral SDW. \mathcal{F}_\uparrow (plain line) and \mathcal{F}_\downarrow (dashed line) are built from truncated sphere plus a small cylinder. A perturbed spin-up state is a superposition of a spin-up plane wave $e^{i\mathbf{k}\mathbf{r}}$ with a spin-down plane wave $e^{i(\mathbf{k}+\mathbf{Q})\mathbf{r}}$ with $Q = 2(1 - \epsilon + h\epsilon)$.

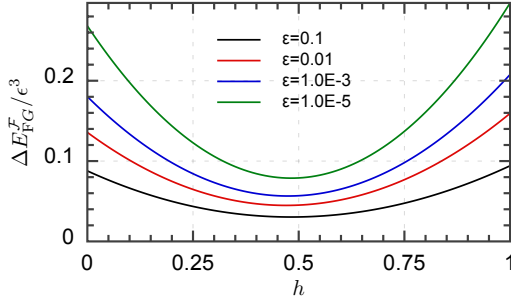


FIG. 2: $\Delta E_{\text{FG}}^{\mathcal{F}}$ as a function of h for different values of ϵ at $r_s = 4$.

$\hbar^2/(ma_B^2))$ is

$$E_{\text{FG}}^{\mathcal{F}} = \frac{a_K R^5}{r_s^2} K_{\text{FG}} - \frac{a_V R^4}{r_s} V_{\text{FG}} \quad (1)$$

$$K_{\text{FG}} = \int_{\mathcal{F}_\uparrow + \mathcal{F}_\downarrow} d\mathbf{k} k^2 \quad (2)$$

$$V_{\text{FG}} = \int_{\mathcal{F}_\uparrow \times \mathcal{F}_\uparrow + \mathcal{F}_\downarrow \times \mathcal{F}_\downarrow} d\mathbf{k} d\mathbf{k}' \frac{1}{|\mathbf{k} - \mathbf{k}'|^2} \quad (3)$$

with $a_V = \frac{3}{32\pi^3} \left(\frac{9\pi}{4}\right)^{1/3}$, $a_K/a_V = 2\pi^2 \left(\frac{9\pi}{4}\right)^{1/3} \approx 37.9$.

The energy change, $\Delta E_{\text{FG}}^{\mathcal{F}}$, can be computed by direct integration (see Fig.2) and gives at the leading order in ϵ [13]:

$$\Delta E_{\text{FG}}^{\mathcal{F}} \approx \frac{2\pi^2 a_V \epsilon^3}{r_s} \left[\alpha(\gamma - 1) - \frac{1}{9} + h \right] \quad (4)$$

with $\alpha = 2(h - \frac{1}{2})^2 + \frac{1}{6}$ and $\gamma = \ln \frac{2}{\epsilon} + \frac{a_K}{a_V \pi r_s}$. For small r_s , ϵ is small and thus γ is large. The minimum of $\Delta E_{\text{FG}}^{\mathcal{F}}$ with respect to h is for $h = \frac{1}{2} - \frac{1}{4(\gamma-1)} \approx \frac{1}{2}$, and, for small r_s , $\Delta E_{\text{FG}}^{\mathcal{F}}$ is four times smaller than in the Overhauser case ($h = 0$).

The spin density waves. In a second step, the SDW are obtained by replacing a plane wave $|\mathbf{k}, \uparrow\rangle$ by $a_{\mathbf{k}} |\mathbf{k}, \uparrow\rangle + b_{\mathbf{k}} |\mathbf{k} + \mathbf{Q}_{\mathbf{k}}, \downarrow\rangle$ ($|a_{\mathbf{k}}|^2 + |b_{\mathbf{k}}|^2 = 1$), for \mathbf{k} in \mathcal{F}_\uparrow . Symmetrically, for \mathbf{k} in \mathcal{F}_\downarrow , a plane wave $|\mathbf{k}, \downarrow\rangle$ is replaced by the combination $a'_{\mathbf{k}} |\mathbf{k}, \downarrow\rangle + b'_{\mathbf{k}} |\mathbf{k} + \mathbf{Q}_{\mathbf{k}}, \uparrow\rangle$ with $a'_{\mathbf{k}} = a_{-\mathbf{k}}$ and $b'_{\mathbf{k}} = b_{-\mathbf{k}}$. We choose $a_{\mathbf{k}}$ real and positive and in the following we assume that $b_{\mathbf{k}}$'s are also positive and that $b_{\mathbf{k}} < a_{\mathbf{k}}$ [12].

As in Fig.1, $\mathbf{Q}_{\mathbf{k}}$ is such that for \mathbf{k} in \mathcal{F}_\uparrow , $\mathbf{k} + \mathbf{Q}_{\mathbf{k}}$ does not belong to \mathcal{F}_\downarrow , and for \mathbf{k} in \mathcal{F}_\downarrow , $\mathbf{k} + \mathbf{Q}_{\mathbf{k}}$ does not belong to \mathcal{F}_\uparrow . The energy change is given by:

$$\Delta E_{\text{SDW}}^{\mathcal{F}} = \frac{2a_K R^5}{r_s^2} K_{\text{SDW}} - \frac{2a_V R^4}{r_s} V_{\text{SDW}} \quad (5)$$

$$K_{\text{SDW}} = \int_{\mathcal{F}_\uparrow} d\mathbf{k} (\|\mathbf{k} + \mathbf{Q}_{\mathbf{k}}\|^2 - k^2) b_{\mathbf{k}}^2 \quad (6)$$

$$V_{\text{SDW}} = - \int_{\mathcal{F}_\uparrow \times \mathcal{F}_\uparrow} d\mathbf{k} d\mathbf{k}' \frac{(a_{\mathbf{k}} b_{\mathbf{k}'} - b_{\mathbf{k}} a_{\mathbf{k}'})^2}{\|\mathbf{k} - \mathbf{k}'\|^2} + \int_{\mathcal{F}_\uparrow \times \mathcal{F}_\uparrow} d\mathbf{k} d\mathbf{k}' \frac{(a_{\mathbf{k}} b_{\mathbf{k}'} + b_{\mathbf{k}} a_{\mathbf{k}'})^2}{\|\mathbf{k} - \mathbf{k}'\|^2} \quad (7)$$

with $\tilde{k}_z = Q - k_z$ (see Fig.1). Using the linear symmetric operators T^\pm :

$$(T^\pm f)(\mathbf{k}) = \int_{\mathcal{F}_\uparrow} d\mathbf{k}' \left(\frac{1}{\|\mathbf{k} - \mathbf{k}'\|^2} \pm \frac{1}{\|\tilde{\mathbf{k}} - \mathbf{k}'\|^2} \right) f(\mathbf{k}'), \quad (8)$$

Eq.5 rewrites:

$$\Delta E_{\text{SDW}}^{\mathcal{F}} = \frac{4a_V R^4}{r_s} (2(\kappa, b^2) + (T^- a^2, b^2) - (T^+ ab, ab)) \quad (9)$$

where (f, g) is the scalar product $\int_{\mathcal{F}_\uparrow} f g$, and $2\kappa(k) = \frac{a_K R}{2a_V r_s} Q(Q - 2k_z) \geq 0$. In Eq.9 the difference between 1 and R is negligible and in the following we set $R = 1$.

Optimal solution. From the variations of Eq.9 with respect to $b_{\mathbf{k}}$, the optimal function b satisfies:

$$2b\kappa + bT^-(a^2 - b^2) = \frac{a^2 - b^2}{a} T^+ ab \quad (10)$$

Setting $\xi = ab$ and using $b^2 \leq \frac{1}{2}$, $a^2 - b^2 = \sqrt{1 - 4\xi^2}$, Eq.10 rewrites $\xi = J(\xi)$ where:

$$J(\xi) = \frac{1}{2} \frac{T^+ \xi}{\sqrt{(\kappa + T^- \sqrt{1/4 - \xi^2})^2 + (T^+ \xi)^2}}. \quad (11)$$

Thus the point is now to find the fixed points of the operator J . The Fermi gas ($\xi = 0$) is a trivial fixed point. By definition $0 \leq \xi \leq \frac{1}{2}$, and from Eq.11, we see that $0 \leq J(\xi) \leq \frac{1}{2}$. We claim that starting with $\xi = 1/2$ and iterating the process $\xi \rightarrow J(\xi)$ leads to a non-trivial fixed point satisfying:

$$\xi(k_z = Q/2) = \frac{1}{2}. \quad (12)$$

Indeed, by (8) the kernels of T^\pm are positive, thus T^\pm are positivity preserving linear operators: if $\xi \geq \xi'$, then $T^+\xi \geq T^+\xi'$; similarly $T^-\sqrt{1/4 - \xi^2} < T^-\sqrt{1/4 - \xi'^2}$, and consequently:

$$\xi \geq \xi' \implies J(\xi) \geq J(\xi'). \quad (13)$$

Thus starting with $\xi_0 = 1/2$, we have $J(\xi_0) \leq \xi_0$ and setting $\xi_n = J(\xi_{n-1})$, ξ_n is a decreasing sequence of positive functions and thus converges to a fixed point ξ_∞ .

1-D approximation. Now we impose that b_k (thus ξ_k) is non zero only in the cylinder \mathcal{C} corresponding to the gray region of Fig.1 where it depends only on k_z : $\mathcal{C} = \{\mathbf{k} : k_x^2 + k_y^2 \leq r^2 = 1 - (1 - \epsilon)^2 \approx 2\epsilon, 0 \leq k_z \leq Q\}$. As we shall see below, b_k differs from zero only in the neighborhood of the top disk of \mathcal{F}_\uparrow (and its symmetric for \mathcal{F}_\downarrow). In any case, these restrictions always provides an upper bound for the energy of the SDW.

First, for the second term of Eq.9, we have:

$$(a^2, T^-b^2) = (b^2, T^-a^2) = (b^2, T^-1) - (b^2, T^-b^2) \quad (14)$$

From Eq.8, $T^-1 = v_{\mathcal{F}}(\mathbf{k}) - v_{\mathcal{F}}(\tilde{\mathbf{k}})$ where $v_{\mathcal{F}}$ is the potential induced by the truncated sphere. In the spherical case, the potential of the unit sphere is given by:

$$v(\mathbf{k}) = 2\pi + \pi \frac{1 - k^2}{k} \ln \frac{1 + k}{|1 - k|}$$

In this case, for k close to 1 (\mathbf{k} and $\tilde{\mathbf{k}}$ are close and near the unit sphere and $\tilde{k}_z = 2 - k_z$), $v(\mathbf{k}) - v(\tilde{\mathbf{k}}) \approx -4\pi(1 - k) \log(\frac{1-k}{2})$. This singular behavior is associated to the discontinuity of the density (in \mathbf{k} -space). An analytic solution is provided for the truncated sphere [13]. This solution has the same behavior except that $1 - k$ has to be replaced by the distance of \mathbf{k} to the discontinuity of the density, i.e. the top disk of \mathcal{F}_\uparrow :

$$(T^-1)(\mathbf{k}) \approx -4\pi(Q/2 - k_z) \log\left(\frac{|Q/2 - k_z|}{2}\right) \quad (15)$$

provided that $|Q/2 - k_z| \ll 1$. For $h > 0$, Eq.15 is still valid[13] except in a small neighborhood of the edge of the top disk. In the following we neglect this effect and apply Eq.15 also for $h > 0$.

Using the scaled distance $x = (Q/2 - k_z)/r$,

$$2\kappa + T^-1 = 2\pi r(\gamma x - 2x \log(x)), \quad (16)$$

and integrating over $\mathbf{q} = (k_x, k_y)$, Eq.9 becomes:

$$\Delta E_{\text{SDW}}^{\mathcal{F}} = \frac{4\pi a_V r^4}{r_s} \delta E_{\text{SDW}}^{\mathcal{F}} \quad (17)$$

$$\delta E_{\text{SDW}}^{\mathcal{F}} = 2\pi(\gamma x - 2x \log(x), b^2) - (T^-b^2, b^2) - (T^+\xi, \xi) \quad (18)$$

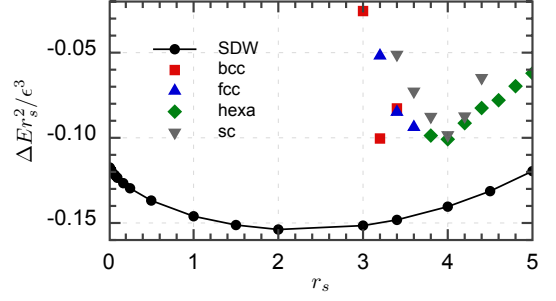


FIG. 3: Renormalized energy $\Delta E r_s^2 / \epsilon^3$ as a function of the density. The dashed-dotted line stands for the analytical solution: $\Delta E r_s^2 / \epsilon^3 = -0.115$. \blacktriangle stand for the SDW simulations. Others symbols stand HF energies (see Fig.5 of [6]).

where the scalar product is now $(f, g) = \int_{x>0} dx f(x)g(x)$, and T^\pm become in terms of x :

$$(T^\pm f)(x) = \pi \int_0^{1/r} dx' (G(x - x') \pm G(x + x')) f(x') \quad (19)$$

$$G(x) = \frac{1}{\pi^2 r^2} \int_{q^2, q'^2 < r^2} d\mathbf{q} d\mathbf{q}' \frac{1}{r^2 x^2 + (\mathbf{q} - \mathbf{q}')^2} \quad (20)$$

$$= 2 \ln \left[1 + \frac{2}{|x|u} \right] - \frac{4}{u^2}, \quad u = |x| + \sqrt{x^2 + 4} \quad (21)$$

In fact, for small r_s , the term (T^-b^2, b^2) may be neglected in Eq.18 [13]. In any case, since T^- is a positive operator, we get an upper bound for the energy and the variation of the resulting upper bound leads to $\xi = J\xi$ where J is now an operator on the positive functions on \mathbb{R}^+ :

$$J(\xi) = \frac{1}{2} \frac{T^+\xi}{\sqrt{\pi^2 (\gamma x - 2x \log(x))^2 + (T^+\xi)^2}}. \quad (22)$$

As above, the fixed point of Eq.22 can be easily found by iteration.

Thereafter, for fixed r_s the total energy variation $\Delta E(\epsilon, h) = \Delta E_{\text{FG}}^{\mathcal{F}}(\epsilon, h) + \Delta E_{\text{SDW}}^{\mathcal{F}}(\epsilon)$ is computed and optimized with respect to ϵ . For $r_s = 3$ about 20 iterations of the operator J are required and about 100 iterations for $r_s = 0.01$ (see \blacktriangle symbols in Fig.3). In the next paragraph, we give a solution for ξ at small r_s and deduce the scaling of ΔE from it.

Analytic solution for small r_s . For small r_s , γ is large and Eq.22 can be solved approximately [13]:

$$\xi(x) \approx \frac{1}{2\sqrt{\frac{x^2}{x_0^2} + 1}} \cos\left(\sqrt{\frac{2}{\gamma'}} \operatorname{arcsinh}\left(\frac{x}{x_0}\right)\right) \quad (23)$$

$$x_0 = 2 \exp\left(-\frac{\pi}{2\sqrt{2}} \sqrt{\gamma'} - \frac{1}{2}\right) \quad (24)$$

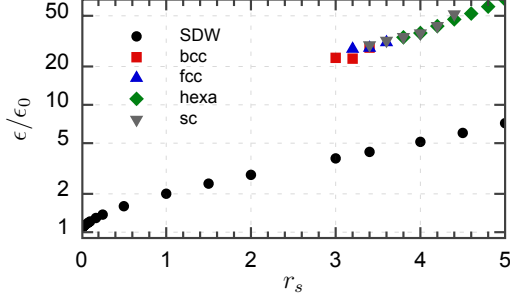


FIG. 4: Scaled parameter ϵ/ϵ_0 as a function of the density. ϵ_0 is the value of Eq.28 for $h = 1/2$. The black circles stands for the present work, while other symbols stand for HF results[6].

for $2\pi\sqrt{2}(\gamma' - \gamma) = \sqrt{\gamma}(\pi^2 + 4)$, leading to the asymptotic behavior of $\Delta E_{\text{SDW}}^{\mathcal{F}}$:

$$\Delta E_{\text{SDW}}^{\mathcal{F}}(\epsilon) \lesssim -C \frac{2\pi^2 a_V}{r_s} \epsilon^2 \gamma \exp\left(-\frac{\pi}{\sqrt{2}}\sqrt{\gamma}\right) \quad (25)$$

with $C = 8e^{-3/2 - \pi^2/8}$.

Now Eq.4 and Eq.25 provide the behavior of $\Delta E(\epsilon, h)$:

$$\begin{aligned} \Delta E &= \Delta E_{\text{SDW}}^{\mathcal{F}} + \Delta E_{\text{FG}}^{\mathcal{F}} \\ &= \frac{2\pi^2 a_V \gamma \epsilon^2}{r_s} \left(\epsilon \alpha - C \exp\left(-\frac{\pi}{\sqrt{2}}\sqrt{\gamma}\right) \right) \end{aligned} \quad (26)$$

The minimum energy is at $\epsilon = \epsilon_0(1 + O(\sqrt{r_s}))$:

$$\Delta E \approx -\frac{\pi a_K \alpha}{r_s^2} \epsilon^3 \quad (27)$$

$$\epsilon_0 = \frac{2C}{3\alpha} e^{-\pi^2/4 - \pi\sqrt{\gamma_0/2}} \approx \frac{0.0294 e^{-7.714/\sqrt{r_s}}}{\alpha} \quad (28)$$

where $\gamma_0 = a_K/(a_V \pi r_s)$. Eq.27 shows that at small r_s , $\Delta E r_s^2/\epsilon^3$ goes to a constant. Fig.3 shows the numerical results for the scaled energy at $h = 1/2$ (\blacktriangle symbols). This scaled energy is of order of -0.1 over a wide range of r_s . On the other hand, while ϵ_0 , Eq.28, varies over decades when r_s decreases, Fig.4 shows that the ratio ϵ/ϵ_0 is a slowly varying function. The analytical result is supposed to be relevant for large γ that is for $\frac{3}{\sqrt{r_s}} \gg 1$. This can be verified on the figure: the next corrections in Eqs.27 and 28 behave as $\sqrt{r_s}$.

Influence of h . The dependency in h is through the parameter α , see Eq.4. Fig.5 shows the effect of h on ϵ and ΔE obtained numerically. For small r_s , at $h = 1/2$ (thus $\alpha = 1/6$), the energy is actually 16 times larger than in the Overhauser model ($h = 0$, $\alpha = 2/3$). At larger r_s , this ratio can be significantly increased, e.g. it is about 200 for $r_s = 5$; in this region we expect the energy gain to deeply rely on the precise shape of \mathcal{F} .

Comparison with HF simulations. In previous HF computations of the jellium[6, 7] we have considered a

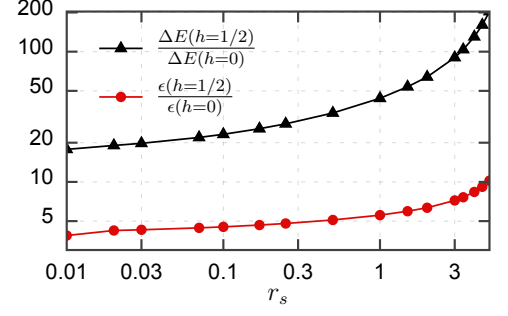


FIG. 5: Influence of h on the energy gain versus r_s : (\blacktriangle) energy and (\bullet) ϵ ratios.

discretized Fermi sphere of 64^3 , 96^3 and 128^3 values of \mathbf{k} . This corresponds to 32, 48 and 64 equally distributed values of k in the interval $(0, 1)$. For $r_s < 5$ evidence for SDW ground states have been found [6]. In Figs 3 and 4, we show the corresponding energy gain per number of SDW (2 for hexa up to 12 for bcc). The larger energy gain of the HF simulations for $r_s \geq 3$ can be mostly attributed to a smoother and better optimized shape, compared to the simple cylinder used in the analytical SDW; other assumptions such as the 1-dimensional approximation decrease the energy further by a factor of 2–3. For $r_s < 3$, the discretization of the Fermi sphere becomes crucial, and even the simulations with 128^3 k-points used in [6] are insufficient to resolve the expected SDW amplitudes leading to the standard Fermi gas ground state ($\epsilon = 0$ and $b_{\mathbf{k}} = 0$). Direct numerical simulations of the SDW in this high density region will require a significant increase of k-points by several order of magnitudes.

Conclusion. Considering the ground state of the jellium in the Hartree-Fock approximation, we quantified the energy of the SDW suggested by Overhauser. Furthermore, we prove that a modification of the truncated Fermi sphere leads to an energy gain 16 to 200 larger than in the Overhauser model.

Our results readily extends to a polarized model : in Eq.7 we have to take into account the direct potential which appears with a factor $1/Q^2$ and thus is negligible at small r_s (of order ϵ^4).

In order to obtain the energy of jellium, the results of Fig.4 must be multiplied by the number of SDW. For simple periodic models considered in previous works, this factor varies from 2 (hexa) up to 12 (bcc). At very small r_s , the perturbation of the SDW is localized in tiny regions which do not interact, thus, one may suppose that we can have many of them distributed around the Fermi sphere giving rise to a quasi-periodic behavior of the density.

-
- [1] S. Huotari, J. A. Soininen, T. Pylkkänen, K. Hämäläinen, A. Issolah, A. Titov, J. McMinis, J. Kim, K. Esler, D. M. Ceperley, M. Holzmann, and V. Olevano, Phys. Rev. Lett. **105**, 086403 (2010).
- [2] A. W. Overhauser, Phys. Rev. Lett. **4**, 462 (1960); Phys. Rev. **128**, 1437 (1962).
- [3] G. F. Giuliani and G. Vignale, *Quantum Theory of the Electron Liquid*, Cambridge University Press, Cambridge (2005).
- [4] S. Zhang and D. M. Ceperley, Phys. Rev. Lett. **100**, 236404 (2008), arXiv:0712.1194 (2007).
- [5] F. G. Eich, S. Kurth, C. R. Proetto, S. Sharma, and E. K. U. Gross, Phys. Rev. **B 81**, 024430 (2010)
- [6] L. Baguet, F. Delyon, B. Bernu, and M. Holzmann, Phys. Rev. Lett. **111**, 166402 (2013), Phys. Rev. **B. 90**, 165131 (2014)
- [7] L. Baguet, PHD thesis, (2014), <https://tel.archives-ouvertes.fr/tel-01127918>
- [8] B. Bernu, F. Delyon, M. Holzmann and L. Baguet, Phys. Rev. **B 84**, 115115 (2011); cond-mat/0810.3559.
- [9] apart from [10], but this estimate is overruled by the present work.
- [10] B. Bernu, F. Delyon, M. Duneau, and M. Holzmann, Phys. Rev. B **78**, 245110 (2008); cond-mat/0810.3559.
- [11] For given ϵ and $0 \leq h \leq 1$, the radius of truncated sphere satisfies $R^3 (4 + 3\epsilon^2(1 - 2h) + \epsilon^3(1 - 3h)) = 4$.
- [12] One easily checks afterwards that the optimal energy is obtained for $b_{\mathbf{k}}$'s with a constant arbitrary phase.
- [13] For detailed demonstrations, see <http://www.lptmc.jussieu.fr/lptmcdata/3DEG/SDW/>